Mathematics Notes
Note 8
14 October 1969

Numerical Inversion of the Fourier Transform

Walter M. Windholz
Kaman Nuclear

The time dependent function f(t) given by the inversion formula

$$f(t) = \frac{1}{2\pi}\int_{-\infty}^{\infty} F(\omega)e^{-i\omega t}\, d\omega \qquad (1)$$

where $F(\omega)$ is the Fourier transform of f(t), is frequently difficult to determine by closed form integration. It then becomes necessary to evaluate the integral in Equation (1) numerically. The objective in this memorandum is to briefly indicate a numerical procedure that yields an acceptable inverse.

1. Some Basic Relationships Between f(t) and $F(\omega)$.

The following relationships between f(t) and $F(\omega)$ are useful relative to the numerical procedure to be discussed later.

1) If f(t) is real then

$$F(\omega) = \int_{-\infty}^{\infty} f(t)e^{i\omega t}\, dt$$

$$= \int_{-\infty}^{\infty} f(t)\cos \omega t\, dt + i\int_{-\infty}^{\infty} f(t)\sin \omega t\, dt \qquad (2)$$

$$= X(\omega) + i\, Y(\omega)$$

where $X(\omega)$ and $Y(\omega)$ are real.

2) If $f(t)$ is real then $f(t)$ is the sum of an even function $f_e(t)$ and an odd function $f_o(t)$, where

$$f_e(t) = \frac{f(t) + f(-t)}{2}, \quad f_o(t) = \frac{f(t) - f(-t)}{2} \tag{3}$$

If $f(t)$ is causal (i.e. $f(t) = o$ for $t > o$)) then

$$f(t) = 2f_e(t) = 2f_o(t) \text{ for } t > o \tag{4}$$

3) Let $F_e(\omega)$ and $F_o(\omega)$ be the Fourier transforms of $f_e(t)$ and $f_o(t)$, respectively. Then

$$F_e(\omega) = \int_{-\infty}^{\infty} f_e(t)e^{i\omega t}\, dt = 2\int_{o}^{\infty} f_e(t) \cos \omega t\, dt \tag{5}$$

$$F_o(\omega) = \int_{-\infty}^{\infty} f_o(t)e^{i\omega t}\, dt = 2i\int_{o}^{\infty} f_o(t) \sin \omega t\, dt \tag{6}$$

Note that $F_e(\omega)$ is real and even while $F_o(\omega)$ is pure imaginary and odd.

4) The function $F(\omega)$ can be written

$$F(\omega) = \int_{-\infty}^{\infty} f(t)\, e^{i\omega t}\, dt$$

$$= \int_{-\infty}^{\infty} [f_e(t) + f_o(t)]e^{i\omega t}\, dt$$

$$= F_e(\omega) + F_o(\omega) \tag{7}$$

It follows from systems (7) and (2) that

$$F_e(\omega) = X(\omega) \qquad F_o(\omega) = i\,Y(\omega) \tag{8}$$

5) In view of system (8) the real function f(t) can be written

$$f(t) = f_e(t) + f_o(t)$$

$$= \frac{1}{2\pi}\int_{-\infty}^{\infty}[F_e(\omega) + F_o(\omega)]e^{-i\omega t}\,d\omega$$

$$= \frac{1}{\pi}\int_{o}^{\infty} F_e(\omega)\cos\omega t\,d\omega - \frac{i}{\pi}\int_{o}^{\infty} F_o(\omega)\sin\omega t\,d\omega$$

$$= \frac{1}{\pi}\int_{o}^{\infty} X(\omega)\cos\omega t\,d\omega + \frac{1}{\pi}\int_{o}^{\infty} Y(\omega)\sin\omega t\,d\omega \tag{9}$$

Similar reasoning applied when f(t) is causal yields

$$f(t) = 2f_e(t) = \frac{2}{\pi}\int_{o}^{\infty} X(\omega)\cos\omega t\,d\omega \tag{10}$$

$$= 2f_o(t) = \frac{2}{\pi}\int_{o}^{\infty} Y(\omega)\sin\omega t\,d\omega \tag{11}$$

6) The function $F(\omega)$ corresponding to a real function f(t) can be written

$$F(\omega) = \int_{-\infty}^{\infty} f(t)e^{i\omega t}\, dt = X(\omega) + i\, Y(\omega) \qquad (12)$$

Differentiation of this system twice with respect to ω yields the relations

$$-iF'(\omega) = \int_{-\infty}^{\infty} tf(t)e^{i\omega t}\, dt = Y'(\omega) - i\, X'(\omega) \qquad (13)$$

$$-F''(\omega) = \int_{-\infty}^{\infty} t^2 f(t)e^{i\omega t}\, dt = -X''(\omega) - i\, Y''(\omega) \qquad (14)$$

Equations (13) and (14) provide the Fourier transforms of the functions $tf(t)$ and $t^2 f(t)$, respectively. Thus,

$$tf(t) = \frac{1}{2\pi}\int_{-\infty}^{\infty} [Y'(\omega) - i\, X'(\omega)]e^{-i\omega t}\, d\omega \qquad (15)$$

$$t^2 f(t) = \frac{-1}{2\pi}\int_{-\infty}^{\infty} [X''(\omega) + i\, Y''(\omega)]e^{-i\omega t}\, d\omega \qquad (16)$$

It should be noted that $X(\omega)$ is even only due to the term cos ωt while $Y(\omega)$ is odd only due to the term sin ωt. It readily follows that $X'(\omega)$ and $Y'(\omega)$ are odd and even, respectively, while $X''(\omega)$ and $Y''(\omega)$ are even and odd, respectively. In view of this Equations (15) and (16) can be written

$$tf(t) = \frac{1}{\pi}\int_{0}^{\infty} Y'(\omega) \cos \omega t\, d\omega - \frac{1}{\pi}\int_{0}^{\infty} X'(\omega) \sin \omega t\, d\omega \qquad (17)$$

$$t^2 f(t) = \frac{-1}{\pi}\int_0^\infty X''(\omega) \cos \omega t \, d\omega - \frac{1}{\pi}\int_0^\infty Y''(\omega) \sin \omega t \, d\omega \quad (18)$$

7) If $f(t)$ is causal then $tf(t)$ and $t^2 f(t)$ are also causal. Thus for $f(t)$ causal and $t < 0$ Equation (17) can be written

$$\int_0^\infty Y'(\omega) \cos \omega|t| d\omega + \int_0^\infty X'(\omega) \sin \omega|t| d\omega = 0 \quad (19)$$

It is immediate from Equation (19) that

$$\int_0^\infty Y'(\omega) \cos \omega t \, d\omega = -\int_0^\infty X'(\omega) \sin \omega t \, d\omega \quad (20)$$

for $t > 0$. It can be shown similarly from Equation (18) that if $f(t)$ is causal and $t > 0$ then

$$\int_0^\infty X''(\omega) \cos \omega t \, d\omega = \int_0^\infty Y''(\omega) \sin \omega t \, d\omega \quad (21)$$

It follows that for causal functions Equations (17) and (18) reduce to

$$tf(t) = \frac{2}{\pi}\int_0^\infty Y'(\omega) \cos \omega t \, d\omega = \frac{-2}{\pi}\int_0^\infty X'(\omega) \sin \omega t \, d\omega \quad (22)$$

$$t^2 f(t) = \frac{-2}{\pi}\int_0^\infty X''(\omega) \cos \omega t \, d\omega = \frac{-2}{\pi}\int_0^\infty Y''(\omega) \sin \omega t \, d\omega \quad (23)$$

2. Numerical Inversion when $F(\omega)$ has no Singularities.

The numerical determination of $f(t)$ will be primarily based on Equation (18) if $f(t)$ is not causal and on Equation (23) if $f(t)$ is causal. It is assumed that the infinite integrals in these equations can be approximated to the desired degree of accuracy with a single finite interval frequency range R given by $\omega_I \leq \omega \leq \omega_F$, $0 \leq \omega_I < \omega_F$, where ω_I and ω_F denote the initial and final values of ω to be considered. The values of ω_I and ω_F are usually determined from the nature of $X(\omega)$ and $Y(\omega)$ relative to mathematical and physical considerations. It is also assumed that $X(\omega)$ and $Y(\omega)$ are sufficiently smooth and do not possess singularities at zero or on the positive real axis.

The functions $X(\omega)$ and $Y(\omega)$ are approximated in the frequency range R by polygonal lines L_x and L_y, respectively, that are defined as follows. Let the range R be divided into subintervals by the set of points ω_n, $0 \leq n \leq N + 1$, where

$$\omega_o = \omega_I, \quad \omega_n < \omega_{n+1}, \quad \omega_{N+1} = \omega_F \tag{24}$$

Also let R_n, $n \geq 1$ denote the frequency range $\omega_{n-1} \leq \omega \leq \omega_n$. The line segments L_n^x, L_n^y that approximate $X(\omega)$, $Y(\omega)$, respectively, on R_n are given by

$$L_n^x(\omega) = \frac{X(\omega_{n-1})[\omega_n-\omega] - X(\omega_n)[\omega_{n-1}-\omega]}{\omega_n-\omega_{n-1}} \tag{25}$$

$$L_n^y(\omega) = \frac{Y(\omega_{n-1})[\omega_n-\omega] - Y(\omega_n)[\omega_{n-1}-\omega]}{\omega_n-\omega_{n-1}} \tag{26}$$

The polygonal lines L_x and L_y can be specified as

$$L_x = \bigcup_{n=1}^{N+1} L_n^x \quad , \quad L_y = \bigcup_{n=1}^{N+1} L_n^y \tag{27}$$

The relationship between L_x and $X(\omega)$ over R is shown schematically in Figure 1 for N = 4. The relationship between L_y and $Y(\omega)$ is schematically similar and thus is not shown here.

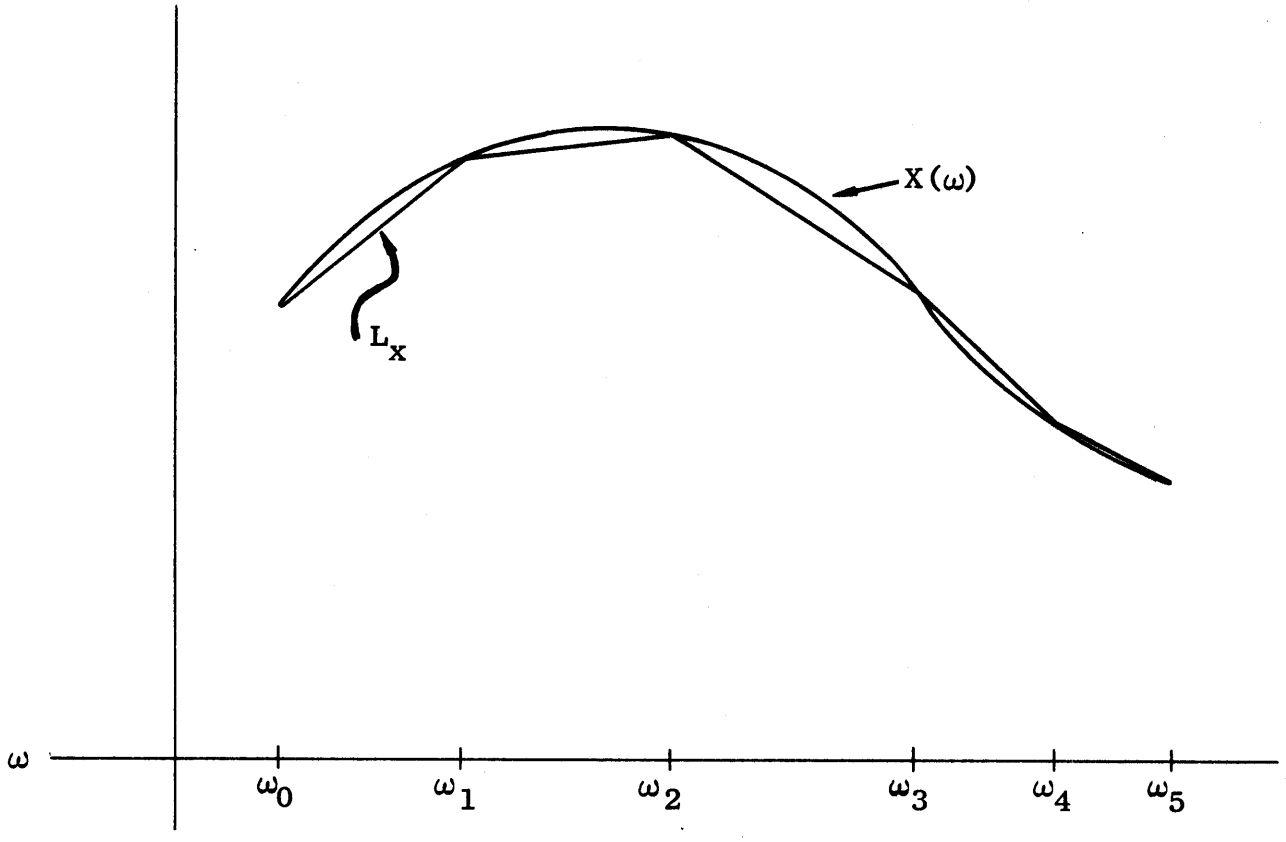

Figure 1. Polygonal Line Approximation to $X(\omega)$.

The first derivatives of L_n^x and L_n^y on R_n are given by

$$\left(L_n^x\right)' = \frac{X(\omega_n) - X(\omega_{n-1})}{\omega_n - \omega_{n-1}} \tag{28}$$

$$\left(L_n^y\right)' = \frac{Y(\omega_n) - Y(\omega_{n-1})}{\omega_n - \omega_{n-1}} \tag{29}$$

These derivatives are the exact derivatives of L_n^x and L_n^y on the open interval $\omega_{n-1} < \omega < \omega_n$ and may be interpreted as right hand derivatives at ω_{n-1} and left hand derivatives at ω_n.

The first derivative that corresponds to the line L^x in Figure 1 is shown schematically in Figure 2. Note that in general the first derivative will have a point of discontinuity at ω_n unless the line segments of the polygonal line corresponding to R_n and R_{n+1} form a single line segment.

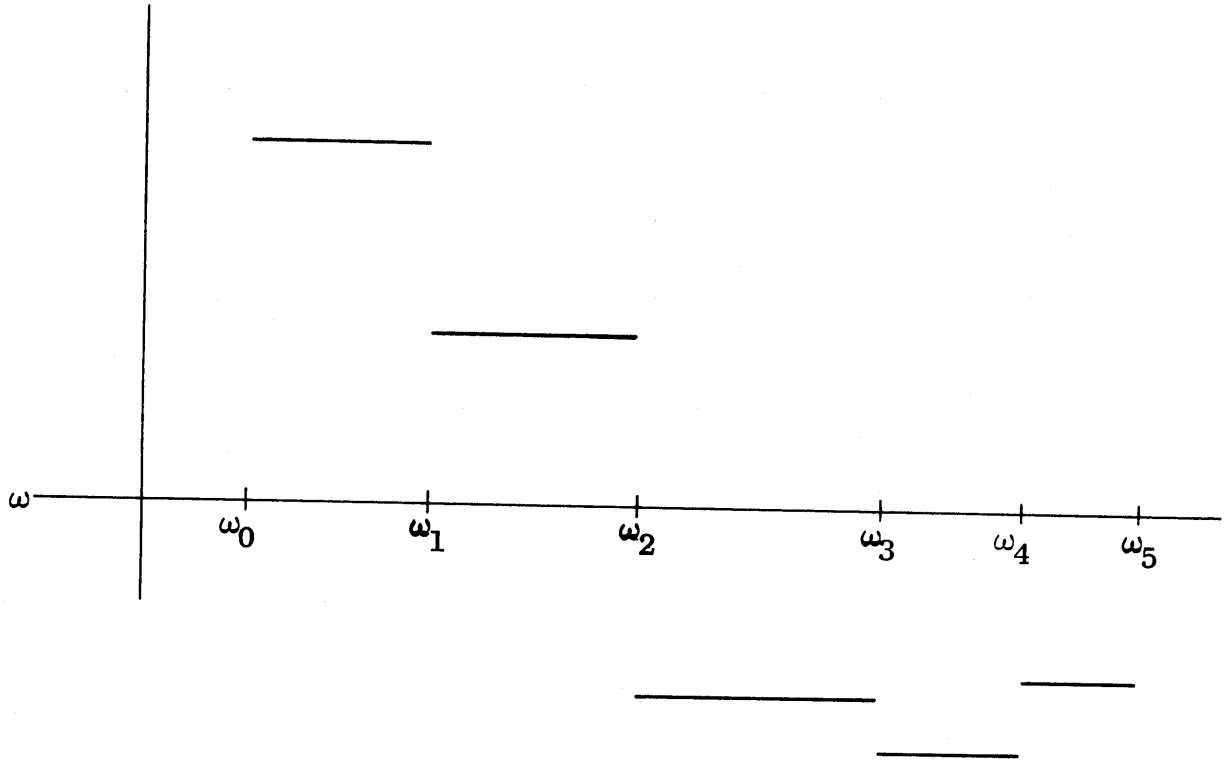

Figure 2. First Derivative of Polygonal Line Approximation.

In order to obtain the second derivative approximations to $X''(\omega)$ and $Y''(\omega)$ the constants C_n^x, C_n^y, $1 \le n \le N$ are first defined as

$$C_n^x = \left(L_n^x\right)' - \left(L_{n+1}^x\right)' \tag{30}$$

$$C_n^y = \left(L_n^y\right)' - \left(L_{n+1}^y\right)' \tag{31}$$

The second derivative approximations to $X''(\omega)$ and $Y''(\omega)$ can be written

$$X''(\omega) \approx \sum_{n=1}^{N} C_n^x \, \delta(\omega-\omega_n) \tag{32}$$

$$Y''(\omega) \approx \sum_{n=1}^{N} C_n^y \, \delta(\omega-\omega_n) \tag{33}$$

where δ is the Dirac delta function. The second derivative approximation corresponding to the schematic representations in Figures 1 and 2 is shown in Figure 3.

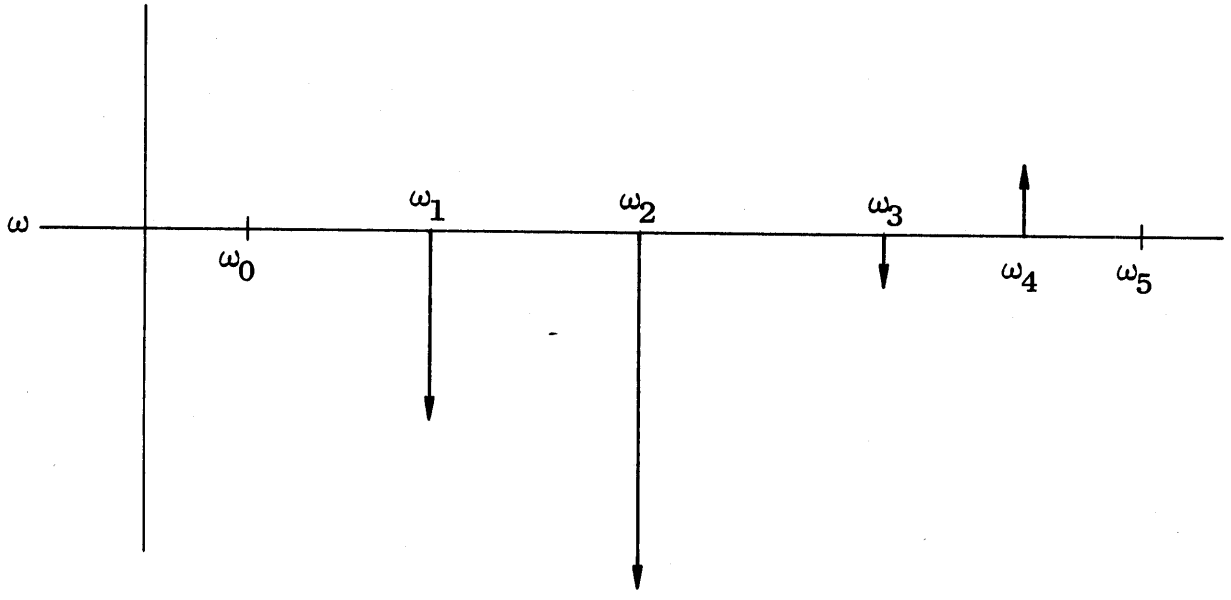

Figure 3. Second Derivative of Polygonal Line Approximation.

Rigorously speaking the derivative of the first derivative of a polygonal line does not exist at the points of discontinuity. The δ function concept may be used however in an approximate limiting sense. For further information on the use of the δ function to approximate derivatives see References 1 and 2.

The δ function has the integration property that if a function, say $g(\omega)$, is continuous on the interval R and ω_n is a point in R then

$$\int_{\omega_I}^{\omega_F} g(\omega)\ \delta(\omega-\omega_n)\ d\omega = g(\omega_n) \tag{34}$$

This integration property can subsequently be conveniently used to determine the function $f(t)$.

Let $f(t)$ be causal. If the approximations for $X''(\omega)$ and $Y''(\omega)$ as given in relations (32) and (33) are substituted appropriately into system (23) the result is

$$t^2 f(t) \approx \frac{-2}{\pi}\int_{\omega_I}^{\omega_F} \sum_{n=1}^{N} C_n^x\ \delta(\omega-\omega_n) \cos \omega t\ d\omega \tag{35}$$

$$\approx \frac{-2}{\pi}\int_{\omega_I}^{\omega_F} \sum_{n=1}^{N} C_n^y\ \delta(\omega-\omega_n) \sin \omega t\ d\omega \tag{36}$$

The integration property of the δ function indicated by Equation (34) can be applied to the approximations (35) and (36) to obtain

$$t^2 f(t) \approx \frac{-2}{\pi} \sum_{n=1}^{N} C_n^x \cos \omega_n t \qquad (37)$$

$$\approx \frac{-2}{\pi} \sum_{n=1}^{N} C_n^y \sin \omega_n t \qquad (38)$$

The numerical approximation to f(t) relative to a given frequency range R becomes better as N is increased.

3. Numerical Inversion when $F(\omega)$ has Singularities.

It may happen that the function $F(\omega)$ corresponding to a real function f(t) has singularities on the non-negative ω-axis. The procedure outlined in the preceding section may become numerically inadequate in the vicinity of the singularities. It then becomes necessary to obtain the numerical inversion of $F(\omega)$ by another numerical procedure that avoids the numerical difficulties encountered near the singularities. Some of these difficulties can be avoided by using the following procedure.

Let $\omega = \nu + i\varepsilon$. Suppose further that the function $F(\omega)$ to be inverted has all its poles below the line $\omega = \nu + ia$, where it is assumed here without loss of generality that $a > 0$. The function $F(\omega)$ may in general have a branch cut along the negative real axis with a branch point at zero. Let C be the contour selected relative to $F(\omega)$ as indicated schematically in Figure 4.

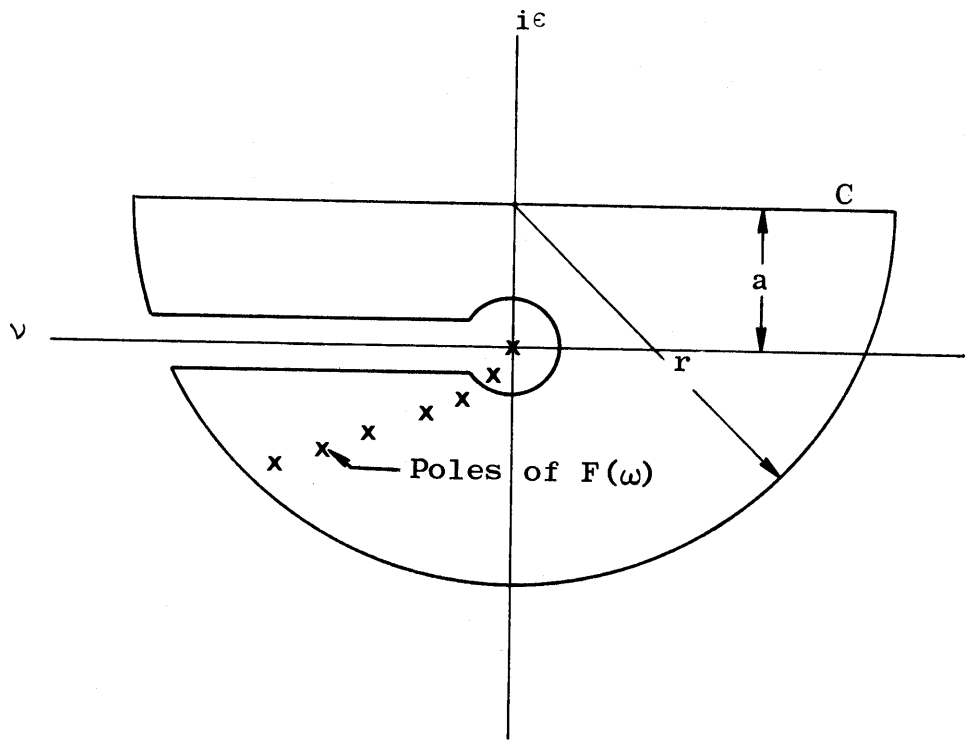

Figure 4. Contour C and Poles of $F(\omega)$ in ω-plane.

It is interesting to examine the image of the contour C in the S-plane, where $S = x + iy$, relative to the mapping $S = h(\omega) = -i\omega$. The mapping h preserves magnitudes but is a rotation through the angle $-\pi/2$. The image C' of C and the images of the poles of $F(\omega)$ under the mapping h are shown schematically in Figure 5.

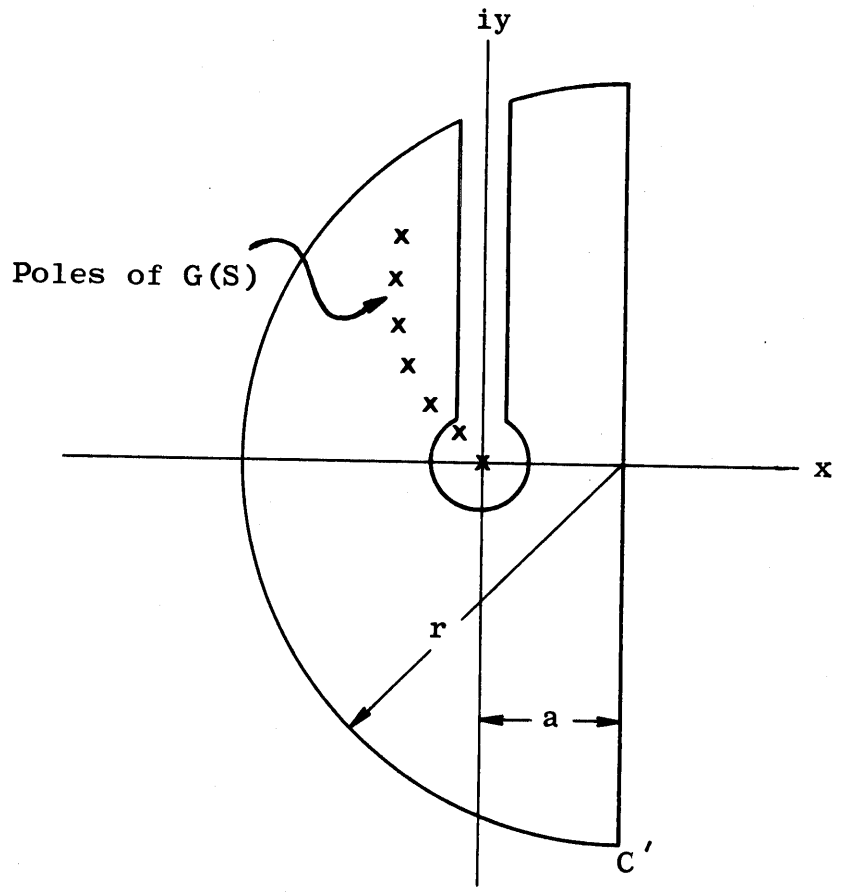

Figure 5. Contour C′ and Poles of G(S) in S-plane.

The function G(S) in the S-plane corresponding to $F(\omega)$ in the ω-plane is given by

$$G(S) = F(iS) = \int_{-\infty}^{\infty} f(t)e^{-St}\,dt \tag{39}$$

If f(t) is a causal function then

$$G(S) = \int_{0}^{\infty} f(t)e^{-St}\,dt \tag{40}$$

It is apparent from system (40) that when f(t) is causal G(S) may be regarded as the Laplace transform of f(t).

The contour C′ in Figure 5 may be regarded as the Bromwich contour associated with the inverse Laplace transformation of G(S) and the causal function f(t) as given by

$$f(t) = \frac{1}{2\pi i}\int_{a-i\infty}^{a+i\infty} G(S)\, e^{St}\, dS \tag{41}$$

provided a is sufficiently large so that all the poles of G(S) lie to the left of the line x = a. In the present context it was assumed that a > 0 without loss of any generality.

Equation (41) can be placed in the ω-plane context by transforming the integral to its equivalent in the ω-plane. Noting that dS = -idω Equation (41) can be written

$$f(t) = \frac{-1}{2\pi}\int_{\infty+ia}^{-\infty+ia} F(\omega)e^{-i\omega t}\, d\omega \tag{42}$$

Since dω = dν + ida = dν on the line ω = ν + ia Equation (42) can be written

$$f(t) = \frac{1}{2\pi}\int_{-\infty}^{\infty} F(\nu + ia)e^{(a-i\nu)t}\, d\nu$$

$$= \frac{e^{at}}{2\pi}\int_{-\infty}^{\infty} F(\nu + ia)e^{-i\nu t}\, d\nu \tag{43}$$

Note that if a = 0 the integral in Equation (43) is the Fourier integral to be evaluated on the real axis. This integration can usually be performed adequately by numerical

integration if $F(\nu)$ is sufficiently smooth on the real axis. If $F(\nu)$ has a singularity on the real axis it is desirable to evaluate the right side of Equation (43) using $a > 0$ and consider this result an approximation to the function $f(t)$ that would be obtained with $a = 0$. Such an approximation could be made as good as desired from an analytical point of view since a can be made arbitrarily close to zero.

Let $A(\Omega,a,t)$ denote the numerical approximation to $f(t)$ in Equation (43), where $a > 0$ and Ω is the set of points ν_n, $0 \leq n \leq N + 1$, on the line $\nu + ia$, that specifies the frequency range of integration and the subdivision used on this range. A very small nonzero value of a does not provide a good approximation $A(\Omega,a,t)$ due to the numerical difficulties encountered in the vicinity of the singularity on the real axis. This remains true even though the span, position and number of points in the set Ω are modified. It can be noted, however, that the only restriction on a in Equation (43) is that $a > 0$; it is otherwise arbitrary. Thus, for $a_1 > 0, a_2 > 0$ and $a_1 \neq a_2$, Equation (43) will yield the same result from an analytical point of view. However, from a numerical point of view $A(\Omega,a_1,t)$ may not equal $A(\Omega,a_2,t)$ for the same set Ω. This is due to the fact that $F(\nu + ia_1)$ may be numerically more suitable on the line $\nu + ia_1$ than $F(\nu + ia_2)$ is on the line $\nu + ia_2$, or vice versa. It appears then that the objective is to find a value of a, large or small, that provides a good numerical approximation $A(\Omega,a,t)$ to $f(t)$, the goodness of the approximation being determined by a criteria to be mentioned later.

In order to determine $A(\Omega,a,t)$ efficiently it is necessary to examine some of the basic properties that relate $F(\nu + ia)$ and $f(t)$ on the line $\omega = \nu + ia$. Suppose $f(t)$ is causal. Then

$$F(\omega) = F(\nu + i\epsilon) = \int_0^\infty f(t)e^{-\epsilon t}\, e^{i\nu t}\, dt$$

$$= \int_0^\infty f(t)e^{-\epsilon t} \cos \nu t\, dt + i\int_0^\infty f(t)e^{-\epsilon t} \sin \nu t\, dt$$

$$= X(\nu,\epsilon) + iY(\nu,\epsilon) \qquad (44)$$

It is readily apparent from system (44) that the real valued functions $X(\nu,\epsilon)$ and the pure imaginary function $iY(\nu,\epsilon)$ are even and odd, respectively, relative to the variable ν.

The approximate inverse $f(t)$ of $F(\omega)$ on the line $\nu + ia$ can be written as

$$f(t) = \frac{e^{at}}{2\pi}\int_{-\infty}^{\infty} [X(\nu,a) + iY(\nu,a)]e^{-i\nu t}\, d\nu$$

$$= \frac{e^{at}}{\pi}\int_0^\infty X(\nu,a) \cos \nu t\, d\nu - \frac{e^{at}i}{\pi}\int_0^\infty iY(\nu,a) \sin \nu t\, d\nu$$

$$= \frac{e^{at}}{\pi}\int_0^\infty X(\nu,a) \cos \nu t\, dt + \frac{e^{at}}{\pi}\int_0^\infty Y(\nu,a) \sin \nu t\, d\nu \qquad (45)$$

Since $f(t)$ is causal Equation (45) can be written

$$f(t) = \frac{2e^{at}}{\pi}\int_0^\infty X(\nu,a) \cos \nu t\, d\nu \qquad (46)$$

$$= \frac{2e^{at}}{\pi}\int_0^\infty Y(\nu,a) \sin \nu t\, d\nu \qquad (47)$$

Here Equations (46) and (47) were obtained using the same kind of reasoning that was used to obtain Equation (20).

The numerical framework used in deriving system (37) can be slightly modified to obtain the appropriate numerical counterparts of the right sides of Equations (46) and (47). The modifications are relatively simple and thus only final results are presented. In particular, for $a > 0$ the numerical counterparts of Equations (46) and (47) are written

$$f(t) \approx A(\Omega,a,t) = -\frac{2e^{at}}{\pi t^2}\sum_{n=1}^{N} C_n^x \cos \nu_n t \qquad (48)$$

$$= -\frac{2e^{at}}{\pi t^2}\sum_{n=1}^{N} C_n^y \sin \nu_n t \qquad (49)$$

where the coefficients C_n^x and C_n^y are now evaluated relative to the point $\omega_n = \nu_n + ia$.

A computer program was written to determine f(t) based on the relationships indicated in systems (48) and (49). This program is called INVERT and is written in Fortran IV for operation on the CDC 6400 computer. At present the program performs the numerical integration relative to the frequency $10^{k_1} \le \nu \le 10^{k_2}$, where k_1 and k_2 are integers that are part of the required input. The number N determines the number of points in this range the convention being that $\nu_1 = 10^{k_1}$, $\nu_N = 10^{k_2}$. The values of ν_o and ν_{N+1} are appropriately adjusted internally in INVERT relative to the numerical procedure used.

The value of a in INVERT is incremented by a uniform increment Δa so that a good approximation can be found. The

approximation $A(\Omega,a,t)$ is considered good if the right side of system (48) equals the right side of Equation (49) to a desired degree of accuracy in the time range of interest. The minimum degree of accuracy required in the practical applications considered to date was agreement to three significant digits.

In the practical applications considered the frequency range of interest was taken as $10^{-10} \leq \nu \leq 10^{9}$. The capability for prescribing the number of increments to be used for a frequency cycle in the range of interest was incorporated into INVERT. It was found that fifty increments/cycle was adequate to yield an acceptable approximation f(t) provided a was made sufficiently large. Here the practical time range of interest was taken as $10^{-9} \leq t \leq 10^{-5}$, where t is measured in seconds. It was noticed that at low values of a, e.g., a = .5 or a = 10, that undesirable oscillation was obtained at very early times. This oscillation was significantly removed when a was assigned values like 1000 or 10,000. The general pattern observed so far was that $A(\Omega,a,t)$ became better as a was increased, it being assumed that Ω remains unchanged. It does not necessarily mean that this pattern will hold for all functions $F(\nu+ia)$ encountered in practical applications. The incremental capability on a in INVERT is designed to help select a satisfactory value of a that will yield an acceptable inverse.

4. Some Specific Numerical Inversions

Among the functions that were inverted was the function $F(\omega)$ that represents the inverse of the transfer impedance of a buried insulated cable. Let r_0 and r_1 denote the radii of the cable conductor and insulator, respectively. Also, let

$$k_1^2 = \mu_1 \epsilon_1 \omega^2$$

$$k_2^2 = \mu_2 \epsilon_2 \omega^2 + i\sigma\mu_2\omega \tag{50}$$

where the subscripts 1 and 2 signify quantities associated with the insulated medium and surrounding medium, respectively. Here the k_j denotes propagation factors, ω denotes frequency, σ denotes conductivity of the surrounding medium, and ϵ_j, μ_j denote the permittivity and permeability of the j^{th} medium.

The transfer function $F(\omega)$ that was inverted can now be written

$$F(\omega) = \frac{F_1(\omega)}{F_2(\omega) + F_3(\omega)F_4(\omega)} \tag{51}$$

where

$$F_1(\omega) = \frac{-8}{k_1 r_1 \omega \mu_2 \pi}$$

$$F_2(\omega) = \left[J_0(k_1 r_0)Y_1(k_1 r_1) - J_1(k_1 r_1)Y_0(k_1 r_0)\right] H_0^{(1)}(k_2 r_1)$$

$$F_3(\omega) = \frac{k_1(\sigma - i\omega\epsilon_2)}{ik_2\epsilon_1\omega}$$

$$F_4(\omega) = \left[J_0(k_1 r_1)Y_0(k_1 r_0) - J_0(k_1 r_0)Y_0(k_1 r_1)\right] H_0^{(1)}(k_2 r_1)$$

The functions $J_n, Y_n, n = 0,1$, are the Bessel functions of the first and second kind, respectively. The Bessel function $H_0^{(1)}$ is the Hankel function of order zero.

The transfer function $F(\omega)$ specified in Equation (51) was inverted using the following input data.

$$r_0 = 1.794 \times 10^{-2} \qquad r_1 = 3.588 \times 10^{-2} \qquad \sigma = 10^{-4}$$

$$\mu_1 = \mu_2 = 1.257 \times 10^{-6} \qquad \epsilon_1 = \epsilon_2 = 3.540 \times 10^{-11}$$

A plot showing graphically the real and imaginary parts of $F(\omega)$ when ω is real is shown in Figure 6 for $10^{-4} \leq \omega \leq 10^{8}$. It is apparent from this figure that $F(\omega)$ is becoming quite large as ω approaches zero. For small ω, $F(\omega)$ behaves as $1/\omega$. Due to this singularity at $\omega = 0$, the inversion of $F(\omega)$ could not be satisfactorily performed on the real axis.

The inverse of $F(\omega)$ was obtained by performing the numerical integration on the lines $\omega = \nu + ia$, where $10^{-10} \leq \nu \leq 10^{10}$ and a had the values 10000 and 20000. The number of increments used per decade on ν was fifty. The inverse $f(t)$, which is the response to a delta function driving pulse, is shown graphically in Figure 7 for $10^{-9} \leq t \leq 10^{-5}$.

The criteria for an acceptable inverse was that the right sides of systems (48) and (49) be nearly equal relative to the numerical framework used. Let $f_1(t)$, $f_2(t)$ denote the inverses obtained using the right sides of systems (48), (49), respectively. Table I shows the results obtained at some times of practical interest. It also provides a comparison between results obtained for a = 10000 and a = 20000.

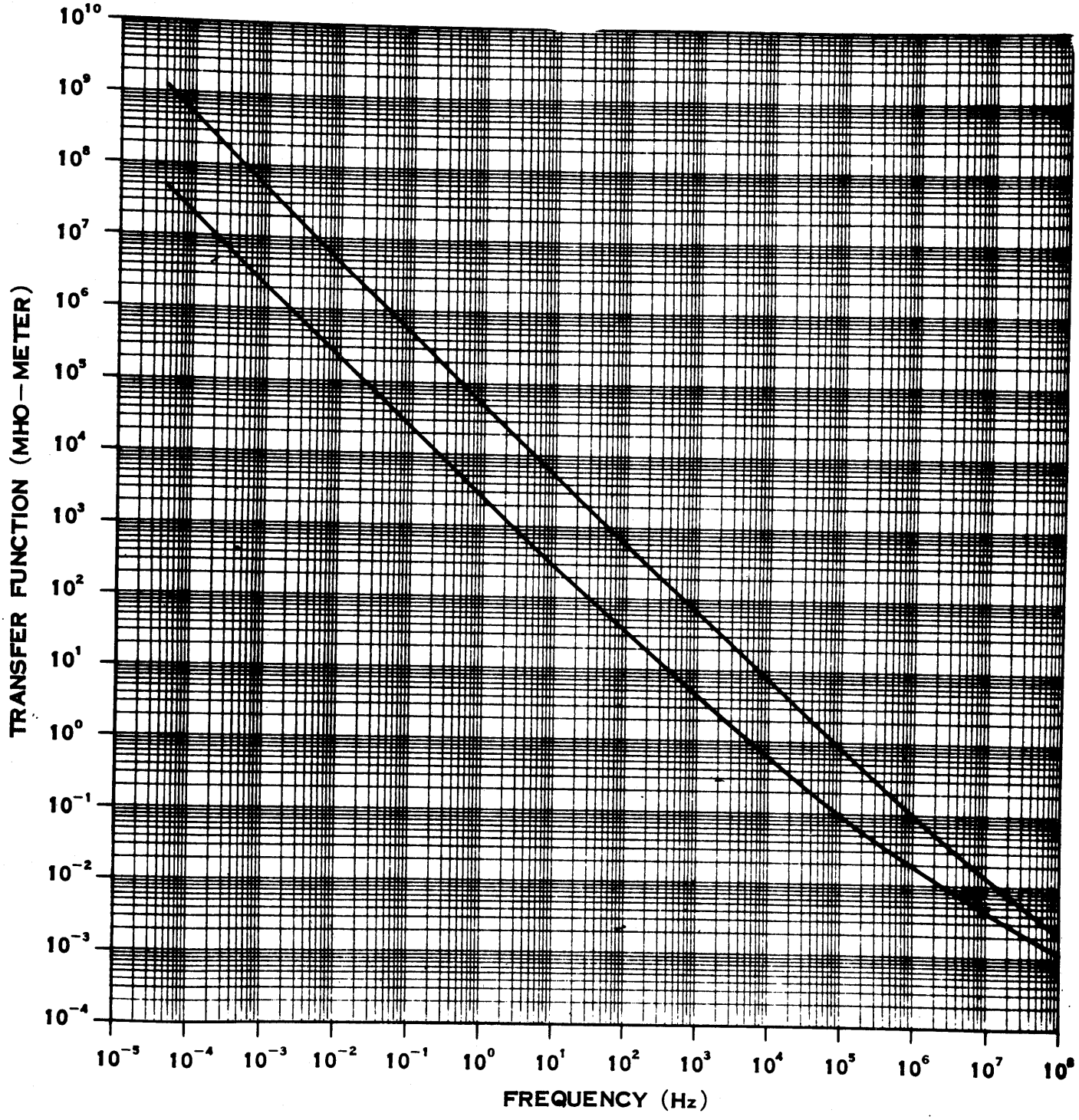

FIGURE 6.

Graph of Transfer Function vs. Frequency

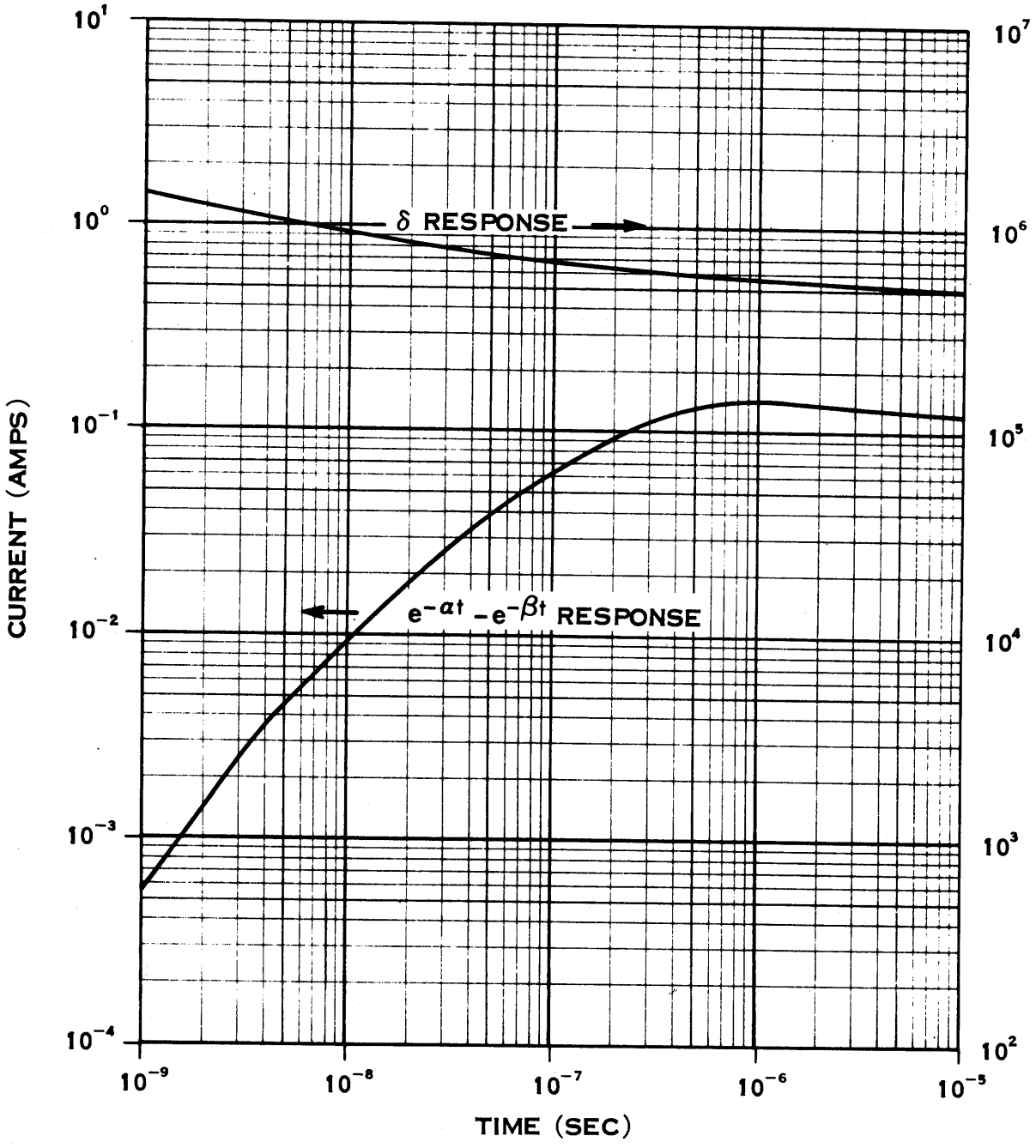

FIGURE 7.

Graph of δ Response and $e^{-\alpha t} - e^{-\beta t}$ Response

TABLE I

RESPONSE OF A BURIED CABLE TO A
DELTA FUNCTION DRIVING FIELD

t (sec)	a = 10000 $f_1(t)$ (amps)	a = 10000 $f_2(t)$ (amps)	a = 20000 $f_1(t)$ (amps)	a = 20000 $f_2(t)$ (amps)
10^{-9}	1.400×10^6	1.398×10^6	1.400×10^6	1.398×10^6
10^{-8}	9.096×10^5	9.096×10^5	9.095×10^5	9.096×10^5
10^{-7}	6.663×10^5	6.663×10^5	6.661×10^5	6.663×10^5
10^{-6}	5.570×10^5	5.571×10^5	5.569×10^5	5.571×10^5
10^{-5}	4.947×10^5	4.948×10^5	4.945×10^5	4.947×10^5

It should be noted that the difference in results at $t = 10^{-9}$ for $f_1(t)$ and $f_2(t)$ disappeared significantly at $t = 2 \times 10^{-9}$. The results at $t = 2 \times 10^{-9}$ were $f_1(t) = f_2(t) = 1.216 \times 10^6$ for both values of a. Additional differences in the results for this time are not known since the results of Program INVERT are presently printed in exponential form with only three digits shown to the right of the decimal point.

The inverse f(t), $10^{-9} \leq t \leq 10^{-5}$, of the function $H(\omega) = E(\omega)F(\omega)$ was also determined, where

$$E(\omega) = \frac{\beta - \alpha}{(i\omega - \alpha)(i\omega - \beta)} \qquad (52)$$

and $F(\omega)$ is the function specified in Equation (51). The values of α and β were 4×10^6 and 4.8×10^8, respectively. The

numerical inversion was performed on the lines $\omega = \nu + ia$, where $a = 10000$, 20000 and $10^{-10} \leq \nu \leq 10^{10}$. The inversion on each line was done using fifty increments per decade. Since $E(\omega)$ is the Fourier transform of $e^{-\alpha t} - e^{-\beta t}$ the time dependent response of the function $h(\omega)$ is referred to as the $e^{-\alpha t} - e^{-\beta t}$ response in Figure 7. The numerical inversion on each line considered was quite adequate relative to the numerical criteria used for determining an acceptable inverse.

REFERENCES

1. Papoulis, Athanasios, "The Fourier Integral and its Applications," McGraw-Hill Book Company, Inc., New York, 1962.

2. Guillemin, E. A., "Theory of Linear Physical Systems," John Wiley and Sons, Inc., New York, 1963